AD-A063 937 SPERRY RESEARCH CENTER SUDBURY MASS F/G 20/5
DISTRIBUTED FEEDBACK SEMICONDUCTOR INJECTION LASER WITH EFFICIE--ETC(U)
NOV 77 H MINDEN F19628-75-C-0178
UNCLASSIFIED SCRC-CR-77-3 RADC-TR-77-397 NL

| OF |
AD A063937

END
DATE FILMED
3-79
DDC

LEVEL II

(12)

RADC-TR-77-397
Final Technical Report
November 1977

DISTRIBUTED FEEDBACK SEMICONDUCTOR INJECTION LASER WITH EFFICIENT FEEDBACK COUPLING

Sperry Research Center

Research was supported by the Air Force In-House Laboratory Independent Research Fund.

ROME AIR DEVELOPMENT CENTER
AIR FORCE SYSTEMS COMMAND
GRIFFISS AIR FORCE BASE, NEW YORK 13441

Dr. H. Minden is the responsible investigator for this contract. Dr. Richard Payne is the RADC Project Engineer.

This report has been reviewed by the RADC Information Office (OI) and is releasable to the National Technical Information Service (NTIS). At NTIS it will be releasable to the General public, including foreign nations.

This technical report has been reviewed and approved for publication.

APPROVED: Richard Payne

RICHARD PAYNE
Project Engineer

APPROVED: Robert M. Barrett

ROBERT M. BARRETT, Director
Solid State Sciences Division

FOR THE COMMANDER: John P. Huss

Plans Office

Unclassified

SECURITY CLASSIFICATION OF THIS PAGE (When Data Entered)

REPORT DOCUMENTATION PAGE

READ INSTRUCTIONS BEFORE COMPLETING FORM

1. REPORT NUMBER: RADC-TR-77-397	2. GOVT ACCESSION NO.
3. RECIPIENT'S CATALOG NUMBER	
4. TITLE (and Subtitle): DISTRIBUTED FEEDBACK SEMICONDUCTOR INJECTION LASER WITH EFFICIENT FEEDBACK COUPLING	5. TYPE OF REPORT & PERIOD COVERED: Final Report, 15 April 1975 – 2 February 1977
	6. PERFORMING ORG. REPORT NUMBER: SCRC-CR-77-3
7. AUTHOR(s): H. Minden	8. CONTRACT OR GRANT NUMBER(s): F19628-75-C-0178
9. PERFORMING ORGANIZATION NAME AND ADDRESS: Sperry Research Center, 100 North Road, Sudbury, MA 01824	10. PROGRAM ELEMENT, PROJECT, TASK AREA & WORK UNIT NUMBERS: 61101F 56380104, 1L1R 5FAA
11. CONTROLLING OFFICE NAME AND ADDRESS: Deputy for Electronic Technology, Hanscom AFB, Massachusetts 01731, Monitor/Richard Payne/ESO	12. REPORT DATE: November 1977
	13. NUMBER OF PAGES: 46
14. MONITORING AGENCY NAME & ADDRESS (if different from Controlling Office): 48p.	15. SECURITY CLASS. (of this report): Unclassified
	15a. DECLASSIFICATION/DOWNGRADING SCHEDULE

16. DISTRIBUTION STATEMENT (of this Report)

Approved for public release; distribution unlimited

5638, 11IR

17. DISTRIBUTION STATEMENT (of the abstract entered in Block 20, if different from Report)

11, 5F

18. SUPPLEMENTARY NOTES

Research was supported by the Air Force In-House Laboratory Independent Research Fund

19. KEY WORDS (Continue on reverse side if necessary and identify by block number)

Gallium Arsenide	Surface Roughness
Diode Laser	Active Layer
Proton Bombardment	Morphology
Liquid Phase Exitaxy	Sliding Boat

20. ABSTRACT (Continue on reverse side if necessary and identify by block number)

Attempts were made to produce a GaAs diode laser structure suitable for bombardment by 200 keV protons. The objective was to bombard the active region through a fine grating mesh in order to produce lasers whose gain varied periodically along the length of the junction.

The requirements for the structure were that the local surface roughness be no more than the order of a wavelength of light, and that the active layer of the structure be within two microns of the surface.

(Continued on reverse side)

DD FORM 1 JAN 73 1473 EDITION OF 1 NOV 65 IS OBSOLETE

Unclassified

20. ABSTRACT (Continued)

Difficulties were encountered in making morphologically acceptable layers. However, the resolution of those difficulties gave insight into the limitations of the sliding boat LPE technique.

Poor device performance was ultimately attributed to the fundamental device structure rather than surface morphology.

EVALUATION

1. This report is the Final Report on the contract. It covers research done on gallium arsenide liquid phase epitaxial structures for injection lasers during the period 15 April 1975 - 2 February 1977. The objective of the research is the development of a distributed feedback laser for use in fiber optic communications and optical signal processing. This phase of the work addresses the problem of growing gallium arsenide epitaxial structures suitable for fabrication of the device. The approach is a new one and offers the potential for improved performance in an integrable laser source.

2. This work provides valuable basic information relevant to fabrication of new and improved optical sources for USAF applications in communications and signal processing.

RICHARD PAYNE
Project Engineer

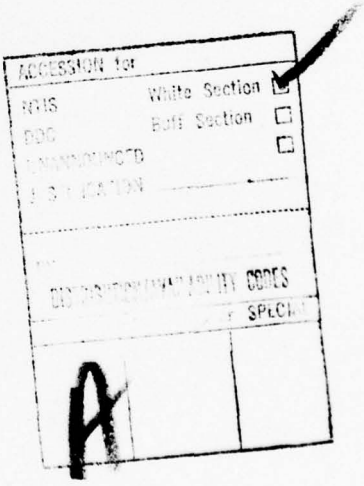

TABLE OF CONTENTS

LIST OF ILLUSTRATIONS

LIST OF ILLUSTRATIONS (Cont.)

SECTION I

INTRODUCTION

Laser diodes, whose active region is in the form of a grating, show promise in integrated optical applications. Such structures are usually prepared by producing periodic variations in the width of either the active layer, or in one of the confining layers of a heterostructure. Thus, in effect, the real part of the propagation constant is varied.

The present project was undertaken to determine whether a grating structure could be made in which the gain or imaginary part of the propagation constant could be varied, and whether such a structure would exhibit the same properties as do conventional gratings.

During the course of some preliminary investigations,[1] it was shown that proton bombardment reduced the number of carriers in GaAs. In particular, the reduction by proton bombardment of the carrier concentration in the active layer of a heterostructure laser was accompanied by a corresponding increase in the threshold. At the same time, there was no decrease in the forward current of the bombarded lasers since the current through the active layer takes place by the diffusion of injected minority carriers rather than by the drift of majority carriers. Annealing restored the free carrier concentration in the active region and lowered the laser threshold to near what they were before bombardment. It was postulated that the increase in threshold resulted from optical absorption by carriers trapped at bombardment induced defects.

The present program was undertaken to discover what combination of bombardment (through a grating mesh) and subsequent annealing would slightly increase the absorption so that the net gain would have a periodic variation of about 10%.

The morphological requirements on the layer structure are fairly severe. The surface roughness over .1mm^2 area (i.e. the area of a laser chip) of the slice must be of the order of the wavelength of light. Moreover, the junction must be within 2μm of the surface for 200keV protons from the bombarder to penetrate to the active region.

The normal double heterostructures require that there be two layers between the active layer and the surface. Table I is a comparison of the various heterostructures discussed in this report. It had been widely mentioned in the literature that it is difficult to make a low resistance ohmic contact to a bare AlGaAs surface. Therefore, a pure germanium doped GaAs contact layer is usually grown on the AlGaAs-Ge confining layer. In all the devices we have made in the past, this layer was 10-20μm thick. Obviously, such a structure could not be used for the bombardment of the active layer by 200keV protons. In our initial work, 2meV protons from a Van de Graaf accelerator were used!

TABLE I

STRUCTURE OF VARIOUS TYPES OF DIODE LASERS

Layer #*	Composition	Impurity	Thickness μm	Function
		Double Heterojunction		
1	$Al_{.2}Ga_{.8}As$	Te (n-type)	1-2	Optical confinement
2	GaAs	Si (n-type)	.2-.5	Active region
3	$Al_{.2}Ga_{.8}As$	Ge (p-type)	1-2	Optical and electron confinement
4	GaAs	Ge (p-type)	2	Contact
		Single Heterojunction		
1	GaAs	Te (n-type)	2	Optical confinement
2	GaAs	Ge (p-type)	1	Active region
3	$Al_{.2}Ga_{.8}As$	Ge (p-type)	1-2	Optical and electron confinement
4	GaAs	Ge (p-type)	1-2	Contact
		Inverted Single Heterojunction		
1	$Al_{.2}Ga_{.8}As$	Ge (p-type)	1-2	Optical and electron confinement
2	GaAs	Ge (p-type)	1	Active region
3	GaAs	Te (n-type)	1-2	Optical confinement and contact

*Layer 1 is next to the substrate or the buffer layer.

To solve the problem of making a shallow junction structure with an ohmic contact, we devised and made the so-called inverted single heterostructure shown in Fig. 1. A pure n-type GaAs-Te single heterostructure confining layer would be used as the surface. Thus, the polarity of the device would be the reverse of the normal polarity. In this structure p-type substrates were not readily available. Instead, we hoped that the junction at the substrate (or at the buffer layer) would be so heavily doped that reverse conduction across it would be by low resistance reverse tunneling.

There were many options initially open to us for the fabrication of the lasers. Homojunction lasers could have been made by diffusion or by vapor phase epitaxy. However, we felt that the ultimate GaAs integrated optics structures would have to be made by LPE. Therefore, we chose this somewhat more difficult technology in preference to the others.

In this program, we encountered two types of problems. The most striking were the problems associated with poor morphology of the layers. The other problems concerned the poor performance of those devices which we were able to make. Throughout the whole course of this investigation, we thought that these two problems were related. We thought that the devices performed badly because the morphology was poor. However, more careful analysis of our complete results indicates that the difficulties which were encountered in making successful lasers could be attributed not to poor morphology, but instead to the fundamental nature of the structure which had been made.

Therefore, the first part of this report will be concerned with the device performance. The results will be presented, and the reason for the poor performance will be described. Changes in the laser fabrication process and device structure will be presented; these changes are logically designed to overcome the difficulty in the basic structure.

Then, because morphology is still an important criterion in the LPE process, it will be discussed in some detail in relation to the results of the present investigation.

Finally, in an Appendix, the LPE apparatus is described in some detail.

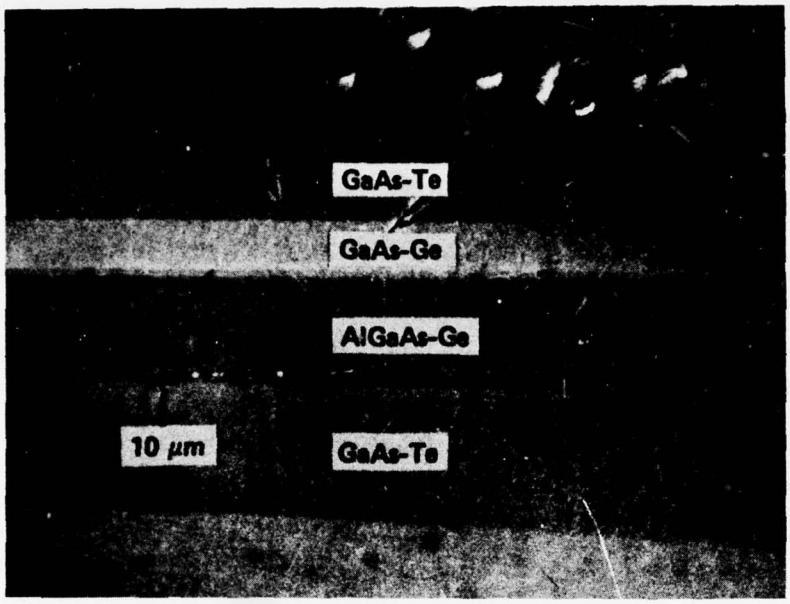

FIG. 1 Photomicrograph of a beveled and stained section of an inverted single heterostructure. Note that a GaAs-Te buffer layer was grown before the AlGaAs-Ge layer. In this early run, the layer thicknesses were a factor of ten larger than required.

SECTION II

DEVICE PROPERTIES

At several stages of this investigation, structures were made which appeared to be satisfactory for making devices. Diodes and even lasers were made from the inverted single heterostructures. Table II is a summary of the properties of some of these devices. However, especially in the case of run 2/5/76, the devices tended to short under the slightest electrical stress. They would short even under examination on the curve tracer. In addition, the laser threshold increased during operation within minutes until threshold could no longer be reached before the device would burn out.

At the time, the relatively high apparent threshold current densities and the tendency of the devices to burn out were attributed to pitting in the various layers and to optical losses at the metal contact. In addition, it turned out that the reverse biased junction at the substrate was rectifying as shown in Fig. 2. We were concerned that heating effects at this junction might have contributed to the device degradation.

At that point in the investigation, we decided to grow conventional double heterostructures without the contact layer. Others have reported that for pulsed operation, it was not difficult to make a satisfactory contact to a bare AlGaAs surface.[2] The AlGaAs would give adequate optical confinement to avoid possible losses at the contact. Moreover, there would be no series rectifying junction and most important the junction would still be close to the surface. Moreover, we reasoned that since we could make both the normal and inverted single heterostructures, we could also make a double heterostructure (DHS). During the attempt to make the DHS, serious problems were encountered with morphology. These will be described and discussed below.

The next successful structures were made towards the end of the program. These were homojunction. Many runs were made which were morphologically sound, and diodes were successfully made from the two slices we tried. Again the diodes burned out under mild stress. Moreover, these diodes were only weak light emitters and there was absolutely no improvement in performance at liquid nitrogen temperature. No laser action was observed.

It was postulated that these devices did not work because there was no carrier confinement in the p-type layer. The p-type layer had been deliberately doped heavily in order to reduce the diffusion length to less than the 1 μm thickness of the p-type layer. The emission wavelength of .91 μm, and the soft reverse breakdown at ~ 5 V attested to the successful heavy doping of both the p and n layers. These devices should have worked at liquid nitrogen temperature; the diffusion length drops off radidly with temperature and there would be no possibility of nonradiative surface recombination.

TABLE II

CHARACTERISTICS OF LASERS
MADE FOR THIS PROGRAM

	Run # 12/17/75	Run # 2/5/76
Weight of Te in buffer layer solution (mg)	138	211
Weight of Ge in AlGaAs layer solution (mg)	523	713
Weight of Ge in active layer solution (mg)	47.2	11.2
Thickness (μm)		
Active layer	1.5	.9
Confining layer	1.5	1
Breakdown voltages		
Reverse	6	12
Forward	2	2
Laser Threshold (kA/cm^2)	14	14
Emission wavelength (Å)	8700	8560

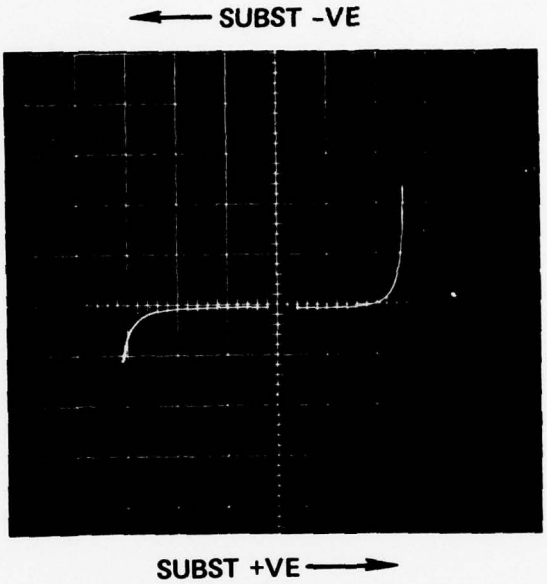

FIG. 2 I-V characteristic of an inverted single heterostructure. The "laser" junction was biased forward to the right. The right hand breakdown is that of reverse biased junction between the GaAs-Te buffer layer and the AlGaAs-Ge confining layer. Horizontal scale 2V/div; vertical scale 1mA/div.

The second homojunction structure had a p-type layer which was doped less heavily, but this did not work either.

Finally, a morphologically sound double heterostructure was made, and diodes were made from this slice. They rectified, but again they shorted under very mild stress. At both room temperature and at liquid nitrogen temperature, they barely gave off light and showed no signs of laser action.

SECTION III

LATERAL RESISTANCE

The reason for the poor device behavior lies in the very structure which was desired. Fig. 3 is a photomicrograph at 200X of the top contact to a chip made for this project. The gold bonding wire was 25μm in diameter and the wire was bonded at several points to the metallized top surface of the chip. The assumption was that the lateral resistance of the contact layer and the top semiconductor layer was small so that the current flow was uniform across the whole area of the junction.

In practice we observed that burn out occurred in the area under the wire bond. This has led us to the conclusion that the lateral resistance of the surface epitaxial layer is large compared to the transverse resistance of that portion of the layer which was directly below the contact. This is illustrated in Fig. 4, where a idealized contact scheme is shown. It can be proved that the ratio of the lateral resistance r_L to the transverse resistance r_T is given by the expression

$$r_L/r_T = (L_o/T)^2 F$$

where

$$F = \ln(L/L_o) \text{ circular case}$$

$$F = L/W \text{ rectangular case}$$

In both cases, F is of the order of unity. However, $L_o \sim 10\mu m$ while $T \sim 1\mu m$. Therefore, for the present structure $R_L/R_T \sim 100$. Note that this ratio is independent of the actual resistivity of the layer.

By contrast, this structure is very different from conventional laser structures. In these structures, the junction has been at least 10 μm from the top surface, and $R_L/R_T \sim 1$! This means that whereas in the former structures the current was indeed uniformly distributed across the junction, in the structures made for this program all the current was confined to the small area under the wire bond.

This condition had two consequences. In the first place, there is the obvious effect of heating. The current density under the contact was a factor of 100 higher than it would have been if the current had been uniformly distributed. This explains why the diodes tended to burn out readily. In addition, heating lowered the quantum efficiency and raised the threshold. Finally, there was the more subtle effect of the absorption losses between the emission region under the contact, and the cleaved facet; these losses contributed to the poor device performance.

In the light of the nature of the lateral resistance, the function of the metallization might be questioned. The metallization in this case does not serve as an electrode.

FIG. 3 Photomicrograph of the top view of a wire bonded chip. The gold wire was .001" in diameter; the bonding wedge had a radius of .0005" and a length of .002". Note how small the contact area was in comparison to the area of the chip.

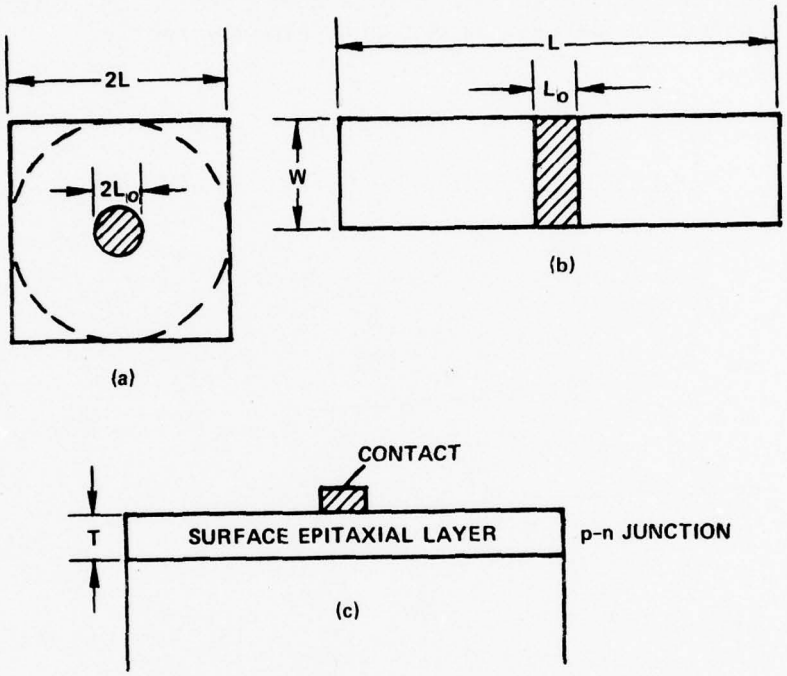

FIG. 4 Schematic diagram of the relationship between the transverse resistance under the wire contact and the lateral resistance of the surface layer radiating from the contact.
(a) Top view of a square chip; (b) top view of a long rectangular chip; (c) cross section of the surface layer and the contact.

The metallization was needed first because wire cannot be bonded directly to bare gallium arsenide; furthermore, the contact between the normal bonding metals, such as gold and aluminum and the semiconductor gallium arsenide, has a high resistance, and is rectifying. The interposition of a specialized metallization was needed for bonding and for low resistance ohmic contact.

Apparently, therefore, the achievement of the required device structure with the junction close to the surface gave rise to the lateral resistance which prevented the devices from functioning correctly.

SECTION IV

LASER FABRICATION

In the light of our understanding of the high lateral resistance of the surface layer, modifications of the laser fabrication process can be suggested. In the first place, it is obvious that the finished device must have a conducting layer, at least 10μm thick, between the wire bond and the junction.

The two micron junction depth is needed only where the protons must penetrate. Thus, a 10μm surface layer with 8μm grooves would be satisfactory. Fig. 5 is a scanning electron micrograph of a raster sputter-etched on a GaAs surface. The periodicity was 4μm and the sputter etch aspect ratio was more than 10:1. The raster pattern was created by contact photolithography in Shipley photoresist, and the photoresist was used directly as the sputter etch mask. This technique is adequate for the 3 μm grating periodicities designed for the present program.

In this structure the current is not confined to the stripes which are not etched. The current under the wire contact which we have been talking about is relative to the chip size. This is of the order of hundreds of microns. The confinement to adjacent stripes 1.5 μm apart would be negligible.

Superficially, the problem seems to be with a wire bond, or more specifically with bonding by means of a pointed tool. The chip might be soldered upside down on the header. There would be the required broad area contact to the junction, and the wire bond would be made to the 200μm thick substrate. In practice, it is very difficult to solder a chip upside down on a header. The solder usually shorts out the junction even when it is a good deal deeper than 1μm. However, the problem of providing a thick, broad area metal electrode has been solved precisely in connection with soldering the chip upside down.[3] The objective in that effort was to provide a broad area heat sink for the junction. In this technique, the surface is metallized as usual and then the thick layer is built up by electroplating. In the present application, the required raster would be created by electroplating or by sputter-etching.[4] Then after the proton bombardment, a gold layer 10-20 μm thick could be electroplated and the chips could be made.

In this way, some of the better slices made for this program can be used to make lasers.

(a)

(b)

FIG. 5 Scanning electron micrograph at 10000X of a raster sputter etched in GaAs. Note the steep aspect ratio of the sides.

SECTION V

MORPHOLOGY

There are four major classes of morphological defects in epitaxial layers grown by liquid phase epitaxy:

1. Pits in the layers were caused principally by the incomplete wetting of the substrate (or previously deposited layers) by the gallium solution. Pitting has also been caused by dissolution of previously deposited layers and by thermal etching of the substrate before deposition.

2. Heavy surface deposition from drops of gallium solution which were carried over from the last deposition. Thus, while at some areas of a slice, wetting may have been incomplete, in other areas the wetting was too great and the boat failed to decant the solution.

3. The surface is always rippled to a greater or lesser extent. This is almost inherent in the process. The deposition temperature is far below the melting point. Many deposition nuclei grow, and the growth rate is rapid and statistically variable. Vapor phase epitaxy produces better morphologies than does liquid phase epitaxy, and epitaxial deposition of silicon is better than that of GaAs.

4. The better the gross surface morphology is, the more readily can subtler defects be observed. Meniscus lines are obviously unique to LPE. Stacking faults occur in LPE grown layers. They are considered serious defects in silicon epitaxial layers, but they were mostly seen in relatively smooth, high quality LPE layers.

Some of these classes of defects will now be discussed in more detail, specifically in relationship to the results of the present program.

PITTING

Fig. 6a is a 2X photograph of a pitted epitaxial layer. Note that the pits were for the most part arrayed in streaks. Fig. 6b shows some of these pits at 1000X. These pits were genuine pits and were not the result of scratches as Fig. 6a might superficially suggest. However, the streaks do imply that the pitting was somehow associated with the motion of the slice in the boat; the streaks were indeed parallel to the direction of boat motion. Moreover, the more intimately the slider was in contact with the boat, or the less the slice clearance was, the more the pits were arrayed in streaks. Finally, the streaked pits were eliminated when a boat made of hard Poco graphite was used. Even then as the hardened graphite surface wore with use, the pits reappeared.

These observations led to the conclusion that there was incomplete or no wetting where graphite particles were abraded onto the GaAs surface. Hot

gallium does not wet graphite; this property is an advantage for boat construction, but obviously clumps of graphite particles on the GaAs surface caused trouble.

It is still uncertain how the particles get onto the GaAs surface. Early in this program, blank experiments were performed in which slices were run through an empty boat at high temperature. There was no significant evidence of particle depostion or oxidation. A possible explanation is that the graphite particles were picked up on the surface of the liquid charges and thus deposited on the surface of the GaAs. There was scant evidence for such a hypotheses. It did seem that the morphology degraded as charges were reused over and over again. However, the statistical evidence for this was unconvincing; there were many spectacular failures with new charges.

Oxygen and oxides of gallium have been blamed for a variety of LPE problems. Certainly, the recent successes of selective LPE show that gallium does not wet SiO_2 deposited on GaAs. Early in the program the system was checked with a helium leak detector, and after simple fixes the system was found to be tight. On the other hand, the system could never by evacuated to a pressure below .02 Torr, even with no boat in the system. Finally, toward the end of the program, appreciable oxide films were noticed at the conclusion of each run. It appeared that after years of use, the hydrogen purifier had finally developed a leak. However, by this time the pitting problem had been eliminated by the use of a new graphite boat.

One problem which may have had something to do with surface wetting and oxidation was the difficulty of depositing an aluminum gallium arsenide layer on a substrate surface. At the time, it was hypothesized that the aluminum in solution reacted with the native oxide on the bare substrate to form aluminum oxide patches on which no semiconductor deposition could take place. The problem was solved by depositing a pure GaAs buffer layer on the substrate. Then the aluminum-gallium arsenide was successfully grown on the in situ prepared surface.

Finally, the occurrence of melt-back gave an appearance of pitting. Fig. 7 is a beveled and stained section of an early run in which there was extensive pitting and melt-back. Note however, that at least the AlGaAs-Ge layer wet the GaAs-Te buffer layer.

DEPOSITION FROM GALLIUM DROPLETS

A drop of gallium solution sometimes appeared on the top of a finished LPE slice. Under the drop was a thick surface layer deposited by the cooling of the solution all the way to room temperature. This layer was not harmful in earlier

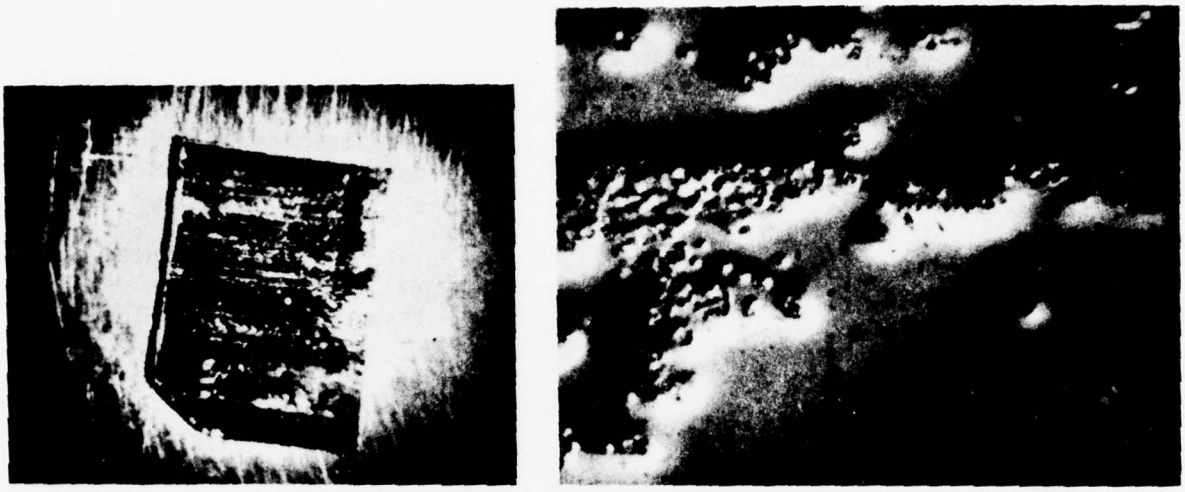

FIG. 6 Streaked arrays of pits in GaAs.
(a) Magnification 2X, (b) Magnification 1000X.

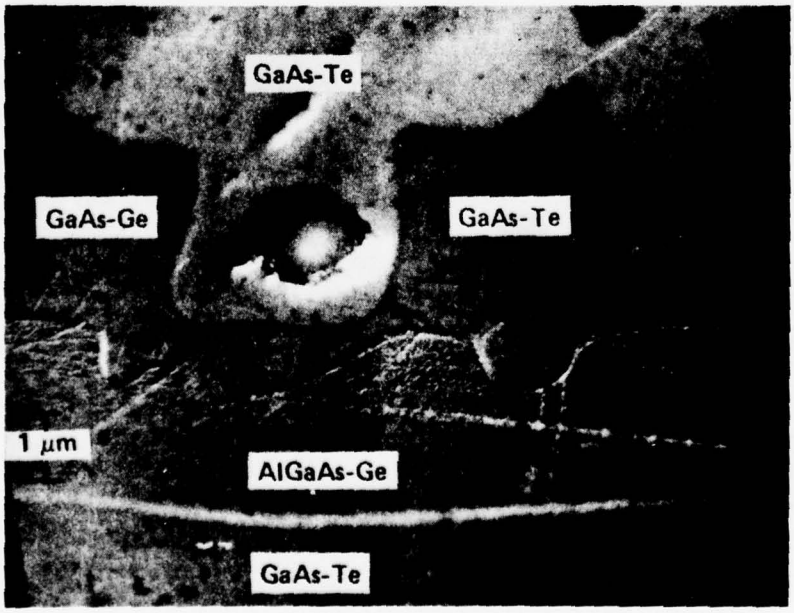

FIG. 7 Beveled section of an early inverted single heterostructure. Complex effects of imperfect wetting and melt-back can be seen.

investigations. For those purposes, a thick contact layer was deliberately grown, and if an even thicker layer protruded over a portion of the surface, it could be gently lapped off.

Fig. 8 is a section showing such a layer. This solution had a high germanium concentration and at low temperatures the germanium finally deposited epitaxially. Such a thick surface layer was obviously undesirable for the purposes of the present program. Moreover, the requirement of a thin surface layer precluded the removal of the thick deposit by lapping and polishing methods.

Many causes have been proposed for solution carryover. For example, the presence of oxides on the surface has been suggested. It is not clear how oxides can prevent and promote wetting at the same time. We have no microscopic explanation for the carryover. However, as might be expected, we did observe that the greater the clearance between the boat and the slider, the greater was the solution carryover. This caused a problem. If the clearance was less than about .003", abrasion caused pitting, while if clearance was greater than about .005" there was excessive solution carryover. Many experiments were done with shims of various sizes between the two halves of the boat.

Part of the problem was that graphite is difficult to machine to close tolerance. It is difficult to assure that the slider will be flat. In fact, the Poco boat was very poorly machined and the slider had to be sanded even to make it slide smoothly over its whole length.

A complicating factor was the dimensional instability of the graphite upon heating. This was especially true of the Poco boat, which warped a different way during each run. A nichrome wire was wrapped around the boat and still there were noticeable gaps between the two halves of the boat after each run, no matter how tightly the halves were bound together.

At this point it became apparent that the Poco boat was not usable. We had been able to make good looking homojunctions. Only two layers and two wells were involved. Moreover, there was no pitting with the Poco boat. However, as noted above, the homojunctions did not laser and it was felt that the heterostructure was required for adequate electron and optical confinement.

The four layer process required that the slice be moved a distance of 8 inches. The warping of the boat was so great that solution carryover was excessive. At this point, it was decided that in order to remedy this problem, extensive modifications would have to be made in the boat design and that such improvements in technology were beyond the scope of the program.

MENISCUS LINES

At the early stages of this work, the appearance of meniscus lines seemed troublesome. Normally these lines were very fine, as shown in Fig. 9,

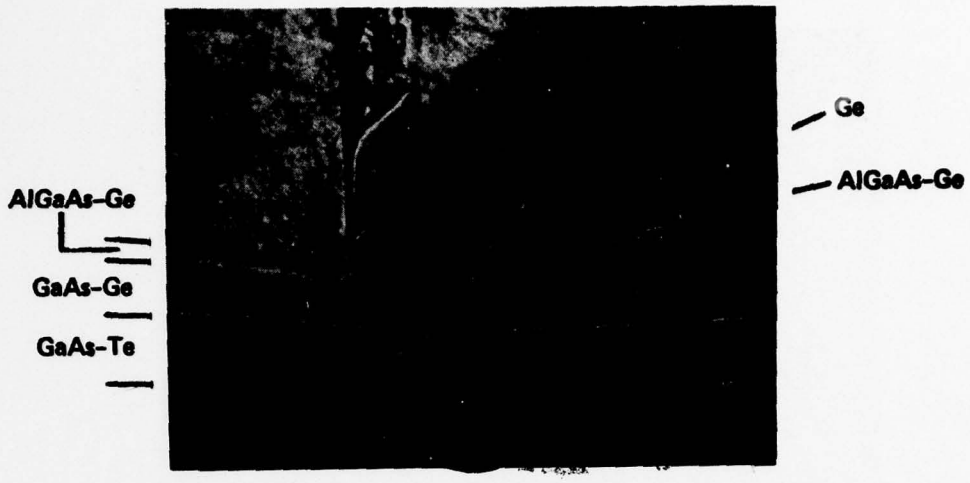

FIG. 8 Section of a single heterostructure at the edge of a thick surface layer. The thick region had been deposited from a drop of gallium solution which had been carried over on the slice from the last well. Note the epitaxial germanium inclusion.

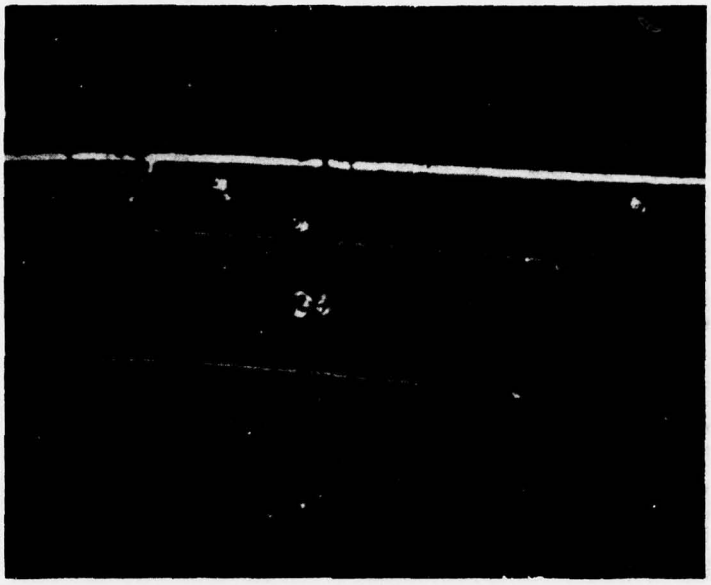

FIG. 9 Photomicrograph under interference contrast at 1000X of fine meniscus lines.

and they were ignored. However, in some runs meniscus lines of a more serious character began to appear. This type of meniscus line is shown in Fig. 10. The lines consisted of grooves or lines of pits. The lines had the characteristic arc shapes associated with LPE menisci.

At the July, 1976, Gordon Research Conference on Crystal Growth, there was considerable discussion of the origin of meniscus lines. Fig. 11 is a schematic diagram of a section of the boat; the diagram illustrates how solution decanting is accomplished in a sliding boat. The formation of the meniscus lines was explained on the basis of the curvature of the liquid-gas interface at the intersection with the solid. The explanation suggested that increasing the clearance between the slice and the boat would reduce the occurrence of meniscus.

These discussions were the origin of our decision to experiment with shimming the two halves of the boat apart. These experiments were successful in that the deep meniscus lines of Fig. 12 were eliminated and the pits were no longer arrayed in streaks.

However, we no longer think that the deep meniscus lines were associated with the curvature of the decanting liquid interface. Instead, as the meniscus sticks and slips, graphite particles flow to the solid-liquid-gas line of intersection. The deep meniscus lines were just another manifestation of the pitting problem.

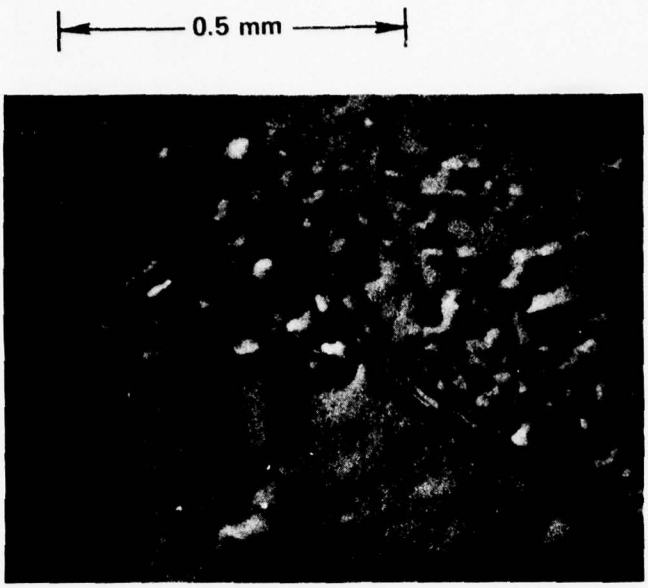

(a)

(b)

FIG. 10 (a) Deep meniscus lines on the surface of the layer. Towards the bottom of the picture the layer was quite smooth. Irregularities were greatly emphasized by the interference contrast illumination.

(b) Beveled and stained section showing how the meniscus grooves on the surface corresponded to places where the active layer didn't grow.

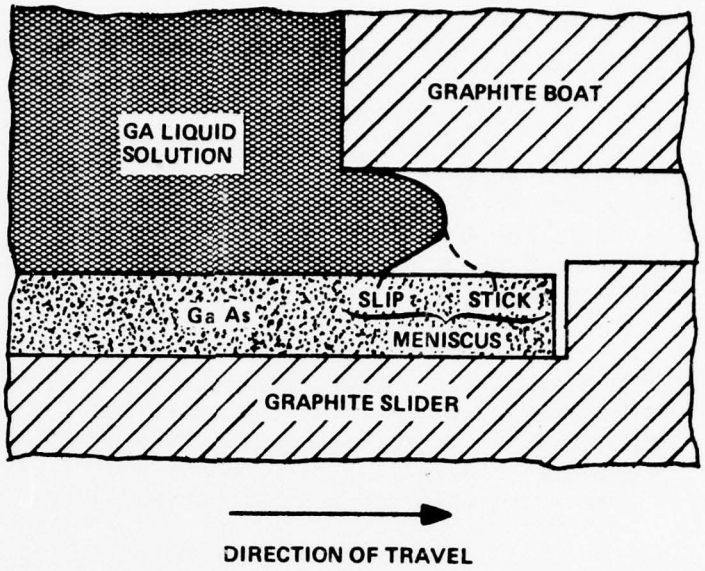

FIG. 11 Greatly enlarged schematic drawing of the part of an LPE boat where the liquid solution makes contact with the GaAs substrate surface. The two critical dimensions are the clearance between the boat and the upper surface of the slice, and the corresponding clearance between the slider and the boat.

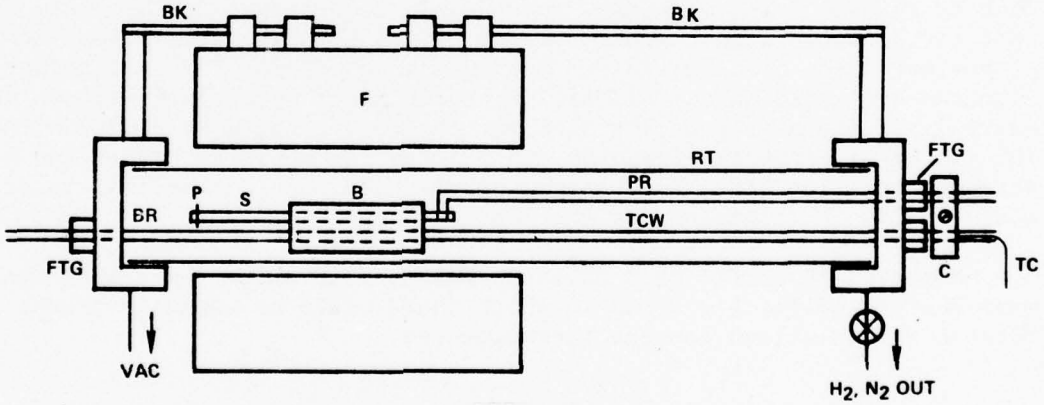

FIG. 12 Schematic of the LPE reactor system. Legend: B- graphite boat; S- slider; F- furnace; RT- reactor tube; EC- end caps; PR- slider pull rod; TCW- combined boat pull rod and thermocouple well; TC- thermocouple rake leads; BR- bucking rod to position the boat in the furnace; P- quartz pin to prevent the slider from being pulled out of the boat. FTG- Cajon O-ring fittings; C- clamp for the pull rod and thermocouple well; BK- support brackets for the end caps.

SECTION VI

BOAT DESIGN

The morphological defects apparently stem from the use of graphite to make the boat. The discussion of the nature of graphite which will be presented in the Appendix leads to the conclusion that graphite which did not warp abraded too easily, while the Poco graphite which resisted abrasion warped. Perhaps a type of graphite may be developed which doesn't warp and nonetheless resists abrasion.

Since such a graphite is not available, the use of quartz as a boat material appears to be attractive. During the course of a very brief investigation, we had considerable success in growing morphologically smooth layers in a quartz sliding boat.[5] In fact, it was on these very smooth layers that meniscus lines were first observed in this laboratory in 1973.

The quartz boat was not used in the present investigation for several reasons. In the first place, aluminum in gallium solution might have attacked the quartz; conceivably this would have destroyed the tolerance in the slider, contaminated the solution and could even have given rise to poor morphology. Secondly, the design of the quartz boat is such that the solutions rather than the substrate are moved with respect to the furnace.[5] The various solution equilibria might have been upset by this change of position in a furnace with uncontrollable temperature gradients. Finally, the quartz boat had no provision for a thermocouple well. Again we were afraid that poor thermal contact between a thermocouple, which would be external to the boat, and the boat itself would lead to poor control of the solution equilbria. However, at present these difficulties do not seem insuperable. A small amount of aluminum dissolved in a 10gm gallium charge might appreciably attack the quartz. If the attack were a problem, the quartz could be coated with a very thin layer of pyrolytic graphite. Such a coating would be harder and more abrasion resistant than bulk compacted graphite, and dimensional tolerance would easily be maintained by the quartz.

Moreover, a quartz boat could be designed in which the slider would move instead of the boat, and in which there would be adequate thermal contact between the solutions and the thermocouples.

APPENDIX

PROCESS DESCRIPTION

OUTLINE

One variation or another of the sliding boat technique is required for the multilayer LPE deposition of III-V compounds. We have used a relatively straight forward adaptation of the technique described by Panish et al.[3] Our boat was unique only in that it accommodated a larger slice than usual.

All the parts of the boat were machined from graphite. The slice was carried in a groove in a long flat slider. The boat proper contained charges in wells. The charges consisted of GaAs and suitable dopants dissolved in gallium. There was a hole drilled in the bottom piece for a thermocouple.

The boat was inserted in a quartz reactor tube inside a furnace. Fig. 12 is a rough sketch of the apparatus. The reactor tube could be evacuated and provision was made for the flow of nitrogen or purified hydrogen. Various rods were inserted through fittings in the end plates of the reactor tube. The boat and the slider were manipulated by means of these rods; one of the rods also served as a thermocouple sheath.

In practice, the charges and the slice were loaded into the boat. The boat was inserted into the reactor tube with the manipulating rods attached. The reactor tube was evacuated and back-filled with hydrogen. The boat was inserted into the furnace and several hours were allowed for the reactants to dissolve in the gallium. The furnace temperature was abruptly lowered to supercool the solutions. The slider was moved to bring the substrate successively in contact with the solutions in each well; the time of contact in each well was determined by the desired thickness of the particular layer. After the deposition was complete, the boat was withdrawn from the furnace and was allowed to cool for at least an hour under hydrogen in the reactor tube. When the boat was cool, the reactor tube was back-filled with nitrogen and the boat was taken out.

The charges were frozen with liquid nitrogen, the boat was dismantled to remove the slice from the slider.

PROPERTIES OF GRAPHITE

Before describing the boat in detail, it is relevant to discuss graphite as a construction material. In the first place, graphite is a bonded compact. Graphite particles are for the most part small flakes, and pure graphite powder does not bond; bulk graphite is not a sintered material. Some other liquid-like material is needed to establish the matrix in which the graphite is held. This is usually the material- such as sugar- from

which the graphite is made. As the sugar is heated, it melts and begins to carbonize. As the carbonization proceeds, and water is driven off the carbon, particles grow but do not necessarily coalesce. The particles are held together by the molasses-like residue from the incomplete carbonization of the graphite. The better the graphite, the less there is of this residue. However, the less there is of the residue, the weaker is the graphite.

The art of graphite manufacture lies in achieving simultaneous purity and strength. Bonding residues have been reduced to a minimum in good graphite, the particle size has been increased, and the porosity has been reduced. Nonetheless, all graphite is soft and abrades easily. There are always pores which become filled with graphite dust.

Gallium does not wet graphite; however, graphite dust readily adheres to the surface of liquid gallium by the forces of surface tension. Where microscopic clumps of graphite dust are interposed between the solution and the substrate, the substrate is not wet and there is no crystal growth. This phenomenon was discussed more fully on page 16. Suffice it to say here, that as a boat is used on successive runs, dust accumulates in the pores and this dust interferes with the LPE process.

Pyrolytic graphite is a non-porous form of graphite; this form is deposited from the gas phase onto surfaces by cracking some hydrocarbon gas. Many years ago it was suggested that pyrolytic graphite be deposited on bonded graphite to seal up the pores of the latter. The Poco Graphite company claims that since pyrolytic graphite has a very anisotropic coefficient of expansion, it spalls off bonded graphite when it is heated. Instead of using pyrolytic graphite to seal the bonded material, the Poco Graphite Company has developed a proprietary pore sealing technique. This involves "impregnating" the surface of the finished, machined piece with a high graphite content liquid under very high pressure. After impregnation, the piece is refined presumably to carbonize the liquid.

We have found this graphite impregnation to be very superficial. After limited use, this surface did abrade. However, the basic graphite was of high quality and the dusting was always less than we have encountered with any other graphite.

On the other hand, the surface stresses induced by the impregnation seemed to be so great that both the boat and the slider warped during the initial firing process and again during use for LPE. The consequences of the warping were discussed on pages 16, 17.

DESCRIPTION OF THE BOAT

Fig. 13 is an engineering print of the boat, and Fig. 14 is a photograph of it. The boat consisted of three parts- the well piece, the base piece and the slider. The well and base pieces dovetailed to form a slot in which the slider could move. The slider itself prevented the boat from

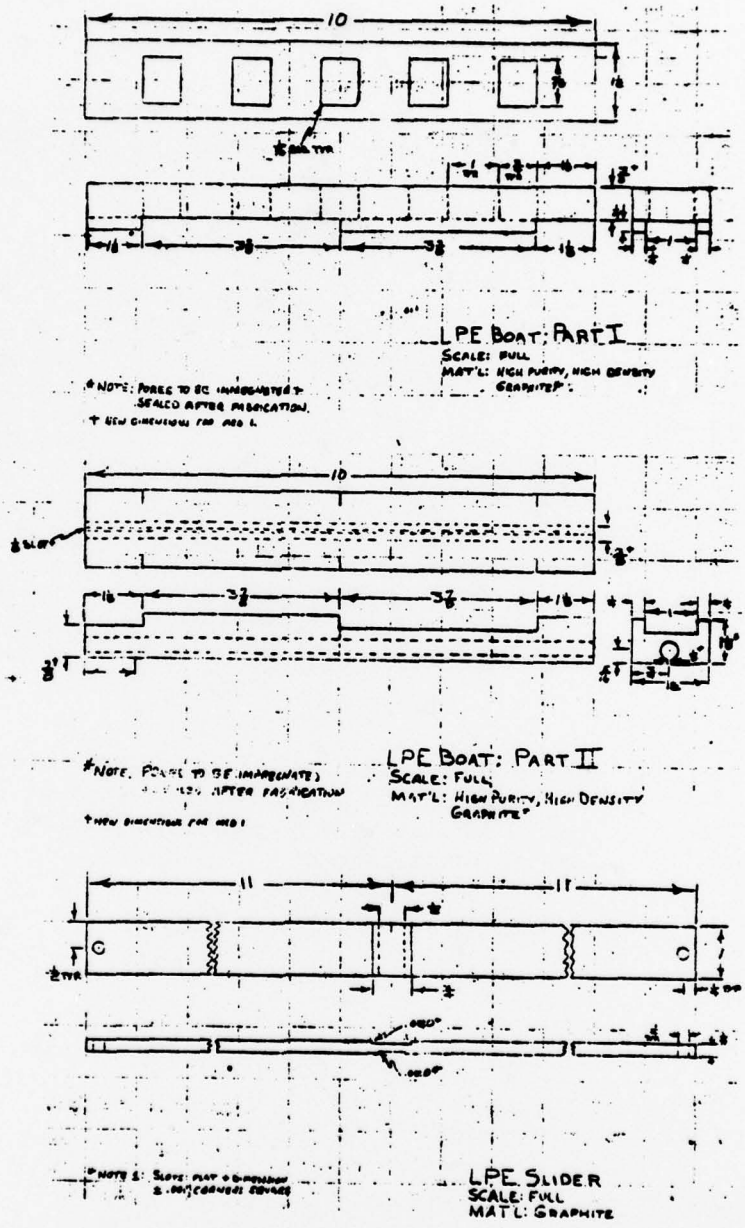

(a)

(b)

(c)

FIG. 13 Engineering print of the LPE boat made by the Poco Graphite Co. (a) Well section. (b) Thermocouple section; note that the thermocouple well ran the length of the boat and was slotted through the bottom. (c) Slider.

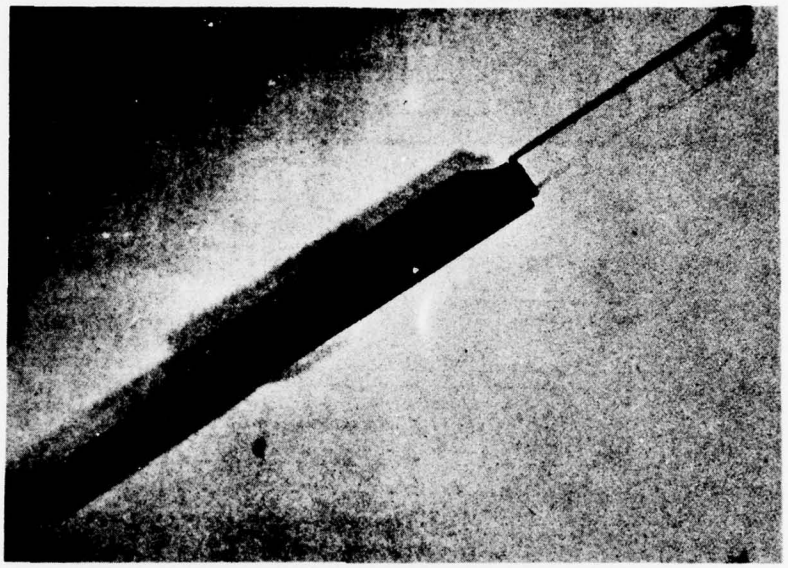

FIG. 14 Photograph of the boat. The slider is at the start position and the back edge of the indexing ruler is even with the leading edge of the slider.

coming apart by lateral motion of the well and base pieces.

The wells were $\frac{3}{4}$" wide while the slider and slices were 1" wide. The $\frac{1}{8}$" overlap of the slice beyond the well was required to prevent the substrate from rising to float on the gallium charge. There is a question as to whether the slice should extend beyond the well in the longitudinal direction as well. There always seemed to be anomalous growth at the edge of the slice, and we feel that the decision is a matter of individual preference and experience.

The base piece had a longitudinal hole to receive a thermocouple well. The hole was longitudinally slotted, as shown in Fig. 13b. The thermocouple well ended in a hook which extended through the slot as the well was being extended with the boat. The thermocouple sheath had a bulge, such that the distance between the hook and the bulge was just the length of the boat. Once the hook cleared the end of the boat, the sheath was rotated. The sheath was sealed at the hook end, and it was long enough to extend through a fitting in the end plate of the reactor tube. Thus, the sheath could be used to move the boat in the reactor tube independently of the position of the slider.

The design and construction of the slider were critical. The substrate groove had to be flat and rounding of the step could not be tolerated. The depth of the slot had to be constant; the bottom of the slot could not be tilted. The slot depth was precisely measured and the back of the substrates lapped to give desired clearances.

The length of the slider was another critical design parameter. If the slider is too long, it will extend outside the hot zone and cool the boat as the slice is moved into the first few wells. The slider can be designed long enough so that the slice can be loaded and unloaded without breaking apart the boat. However, since the substrate groove was open at the sides, the slice tended to slide beyond the edge of the slider as the boat was being pushed into the furnace. Moreover, there was thermal etching of the exposed slice as during soak period. Therefore, the slider was designed just long enough so that when the slider pull rod hook bore against the front of the boat, the slice was just beyond the first well in the back. There were holes in each end of the slider to accommodate the hook of the pull rod and a quartz stop pin. When the pin bore against the back of the boat, the slice was just beyond the front well. (Actually, the Poco machinist broke the slider and we were never able to clear the fifth well. Fortunately, our laser structure never called for more than four wells)

The distance between the edges of each well was 1". This minimized- but did not prevent- carryover of gallium from one well to the next. In addition, we had the option of placing the slice between wells while, for instance, the furnace temperature was being changed.

Fig. 14 also shows how the slider was indexed. The boat was placed on

a bench and the ruler was marked off as the slider was pushed along in simulation of a run. The back end of the ruler was even with the front end of the slider when the hole for the pull rod was tangent to the front end of the boat. This was the zero index point.

Finally, the clearance between the slider and the well piece is critical. This is shown in the detailed sketch of Fig. 11. The morphological consequences of the clearances being too great or too small were discussed on pages 16-19.

REACTOR

The reactor (shown in Fig. 12) consisted of a 58-60mm OD x 150-155cm long quartz tube. The ID of the tube was dictated by the 56mm diagonal section of the boat; even so the corners of the boat had to be chamfered. The length of the reactor tube was dictated by the 75cm length of the furnace combined with the 50cm length of the boat and projecting slider. The reactor tube had to be long enough to permit the boat to be completely withdrawn from the furnace even with the slider fully extended. (Note that some reactor furnaces are on wheels so that the furnace can be removed from around the reactor tube. This places some constraints on the nature of the furnace and the design of the reactor tube; the tradeoff is one of personal preference.)

The ends of the reactor tube were sealed by end caps. These are shown in Fig. 15. The end caps were supported by brackets which were bolted to the top of the furnace. The end caps could be moved longitudinally and also swung laterally out of the way, so that the reactor tube could be removed from the furnace. The end caps actually supported the reactor tube rather than vice-versa.

The end caps consisted of three pieces. The main body held two O-rings and there were ports for vacuum and gas lines. The seal to the reactor tube was made by a large O-ring on the outside of the tube; the O-ring was held under compression between the main body of the end cap and a large bushing bolted to the furnace side of the end cap. This seal was broken only when the reactor tube was removed from the system.

The end caps were finally sealed by end plates which were bolted against O-rings on the outside face of the main body. The end plates had holes to accommodate Cajon brand O-ring fittings for the thermocouple well, the pull rod and the bucking rod.

The arrangement for the manipulators is shown in Fig. 12. The Cajon fittings could be loosened to permit the rods to slide longitudinally, or the fittings could be tightened to make a vacuum seal and also fix the position of the rods and the thermocouple well. Finally, outside the reactor tube, there was a small clamp between the slider pull rod and the thermocouple well. This clamp was tight while the boat was moved in the reactor

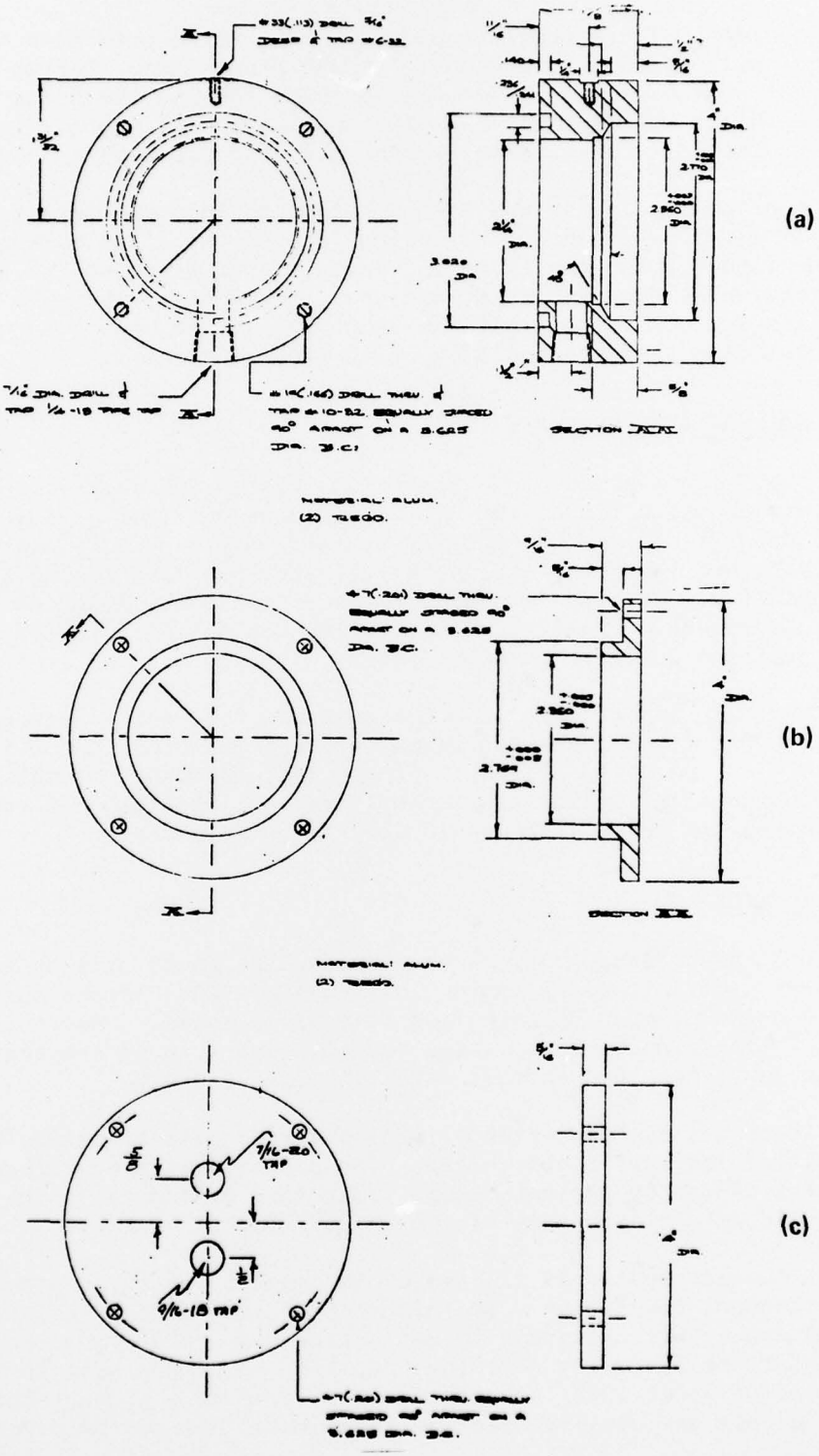

FIG. 15 Engineering drawings of the end caps. (a) Cap body; (b) compression bushing for the main O-ring; (c) typical end plate.

tube by means of the thermocouple well; the clamp prevented the slider from moving, with respect to the boat, at the wrong time. During the run proper, the boat was held fast between the bucking rod and the bulge in the thermocouple well. The fittings on both these rods were tight. To move the slider, the pull rod fitting and the pull rod clamp were loosened.

A piece of tape around the pull rod provided the moving index mark for the slider. The clamp was butted up against the fittings when the boat was in the furnace, and the clamp in this position provided the stationary index mark. The tape was so placed that it coincided with the clamp when the pull rod was pushing against the front end of the boat. As mentioned above, this was made the zero position of the indexing ruler.

GAS HANDLING SYSTEM

Provision was made to evacuate the system and back-fill with nitrogen or hydrogen which flowed through a palladium purifier. Fig. 16 is a schematic diagram of the gas handling system. A pressure regulator and gauge were provided to prevent the back-fill pressure from rising above one pound. A pressure-vacuum gauge was used to ascertain the completion of the back-filling process. Finally, a check valve was provided to isolate the reactor tube from the purifier pumping system.

Hydrogen was flowing when the boat was hot, while nitrogen was used at all other times. The gas flows were not measured, but estimated by the bubbling at the exit oil trap. It was only necessary to maintain the hydrogen flow constant during the temperature equilibration and run proper; otherwise, the temperature would vary uncontrollably.

FURNACE

A standard laboratory three zone Kanthal wound silicon diffusion furnace was used. It had a conventional master-slave temperature controller with continuous proportioning and reset rate modes. However, the thermal mass of the furnace was so large and the time rate of temperature change was so low, that the controls were set quite loosely.

There was also an external single strand potentiometer in the set point circuit of the master controller. The potentiometer was driven through a magnetic clutch by a clock motor. With this arrangement, the furnace could be cooled at a steady rate of $.20^{o}$- $.25^{o}$/min.

A furnace system is limited by the quality of the heater windings and the attendant insulation. In this respect, the furnace zones were unevenly heated and it was difficult to get a zero temperature gradient along the length of the boat. By judicious positioning of the boat in the furnace, a gradient of about $.03^{o}$/inch could be achieved at a given temperature, but this balance was usually upset as the furnace was cooled during a run. The

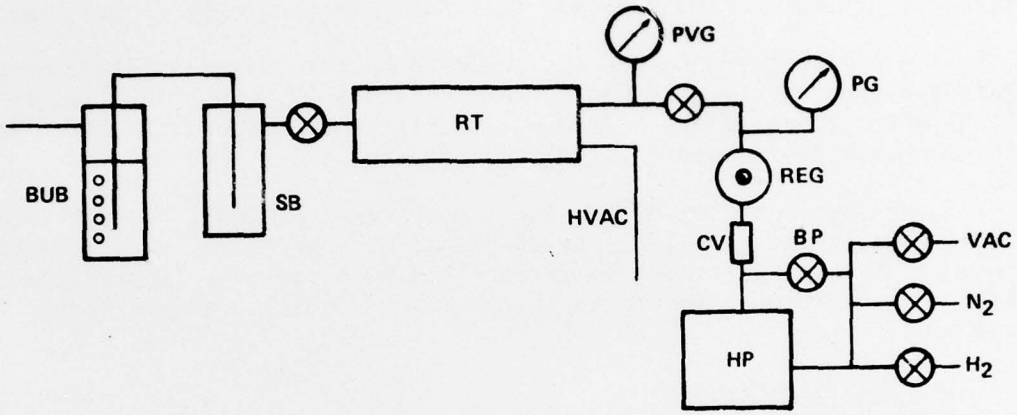

FIG. 16 Schematic of the gas handling system. RT- reactor tube; HP- hydrogen purifier; BP- purifier bypass for the nitrogen; CV- check valve; REG- regulator set to one pound; PG- pressure gauge; PVG- pressure vacuum gauge; VAC- pump for the purifier manifold; HVAC- "high vacuum" for the reactor tube; BUB- oil bubbler; SB- safety bottle.

settings of the slave zones had only a secondary effect on the thermal gradient.

Fig. 17 shows the temperature measurement system. Three thermocouples spaced 4 inches apart were contained in a single .170" OD Inconel sheath. A chromel wire was common and three alumel wires were spot-welded to form a so-called thermocouple rake. The Boonton meter was used not only for the null; the deviation from the null was plotted on a chart recorder. When the VTVM was set on the 100μV range, full scale range on the recorder was 2.5°.

The center thermocouple was centered on the boat and temperature differences and variations could be read to about $\frac{1}{4}$°. No stabilized cold junctions were provided; the system was sensitive to temperature fluctuations in the room air due to drafts, etc.

Care had to be taken with the temperature readings. Garden variety thermocouples are unreliable to within 1° C. Therefore, apparent abrupt temperature gradients must be interpreted with caution. For instance, we felt that our center thermocouple read consistently a degree higher than the end ones.

MATERIALS PREPARATION

Standard high purity materials were used. 99.9999% purity gallium from either Alcoa or Alusuisse was used in the form of individually packaged 10 gm slugs. Substrates were commercially polished, and then were etched and rinsed just before use.

The only unusual requirement was that the substrates be rectangles which fit the groove in the slider. The slices were scribed and cleaved approximately to size and waxed, polished side down, to a glass template. The overlapping edges of the substrate were sanded down to the dimensions of the template.

In some runs, GaAs source slices were weighted down on top of the gallium charges.[4] In the end, when the supercooling technique[5] was adopted, weighed amounts of GaAs were used as the source.

CHARGE COMPOSITION

The charge compositions were determined from published phase diagrams. Calculation of the weight of GaAs was based on the T-x phase diagram of pure GaAs,[6] even though a small amount of aluminum might have been required. Table III is the arsenic concentration of a gallium solution which is in equilibrium with GaAs at various temperatures. The weight of GaAs required is

$$W_{GaAs} = 2.07 \frac{X_{As}}{1-X_{As}} W_{Ga} \qquad (1)$$

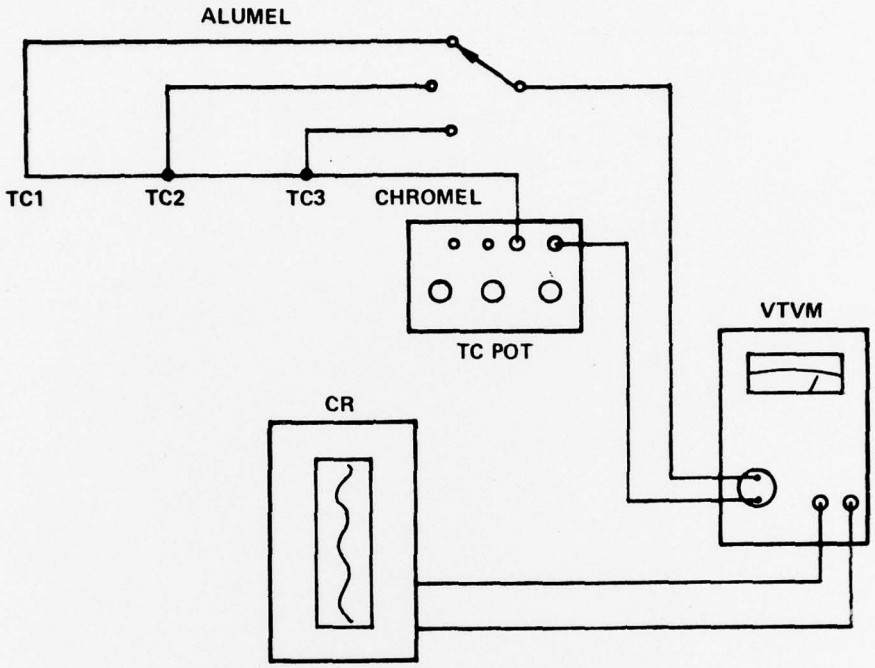

FIG. 17 Schematic diagram of the temperature measurement system. TC1, TC2, and TC3 comprise a three pronged chromel-alumel thermocouple rake. TCPOT- thermocouple potentiometer; VTVM- vacuum tube voltmeter; CR- chart recorder.

TABLE III

EQUILIBRIUM SOLUBILITY OF ARSENIC IN GALLIUM

Temperature °C	Mol Fraction Arsenic
805	.0240
810	.0254
815	.0269
820	.0284
825	.0300
830	.0317
835	.0335
840	.0354
845	.0374
850	.0394

where X_{As} is taken from Table I and W_{Ga} is the weight of the gallium charge. Fig. 18 is the aluminum - $Al_xGa_{1-x}As$ phase diagram[7] where X_{Al} is the mol fraction of aluminum in gallium solution. The weight of aluminum required is

$$W_{Al} = 0.373 \frac{X_{Al}}{1-(X_{Al} + 2X_{As})} W_{Ga} \qquad (2)$$

where X_{Al} is obtained from Fig. 18 and X_{As} from Table III.

The required concentrations of donor and acceptor impurities in solution were also determined from phase diagram data - ultimately modified however, by our own experience. For instance, published data[8] indicate that for tellurium at 850° D., the electron concentration in crystallized GaAs is related to the weight of Te in Ga solution by

$$W_{Te} = 3.6 \times 10^{-23} W_{Ga} n \qquad (3)$$

Eq(3) predicts that only .4 mg Te need be dissolved in 10 gm Ga to achieve an electron concentration of $10^{18} cm^{-3}$. In reality more like 100 mg of Te are required.

On the other hand, the literature value[10] for the hole concentration of germanium doped GaAs (at 900° C) is

$$p = 2 \times 10^{18} X_{Ge} \qquad (4)$$

and

$$W_{Ge} = \frac{X_{Ge}}{1-X_{Ge}} W_{Ga} \qquad (5)$$

To achieve a hole concentration of 10^{18}, the weight of Ga must be of the same order as that of the Ga charge. When drops of the Ga charge were carried on the top surface of the slice, germanium deposited epitaxially on the GaAs as the boat was cooled to room temperature.

Zinc dopes GaAs more heavily than does germanium. However, zinc diffuses rapidly in III-V compounds. As a result, impurity distributions in p-n junctions made with zinc are poorly controlled. In addition, zinc is very volatile during equilibration.

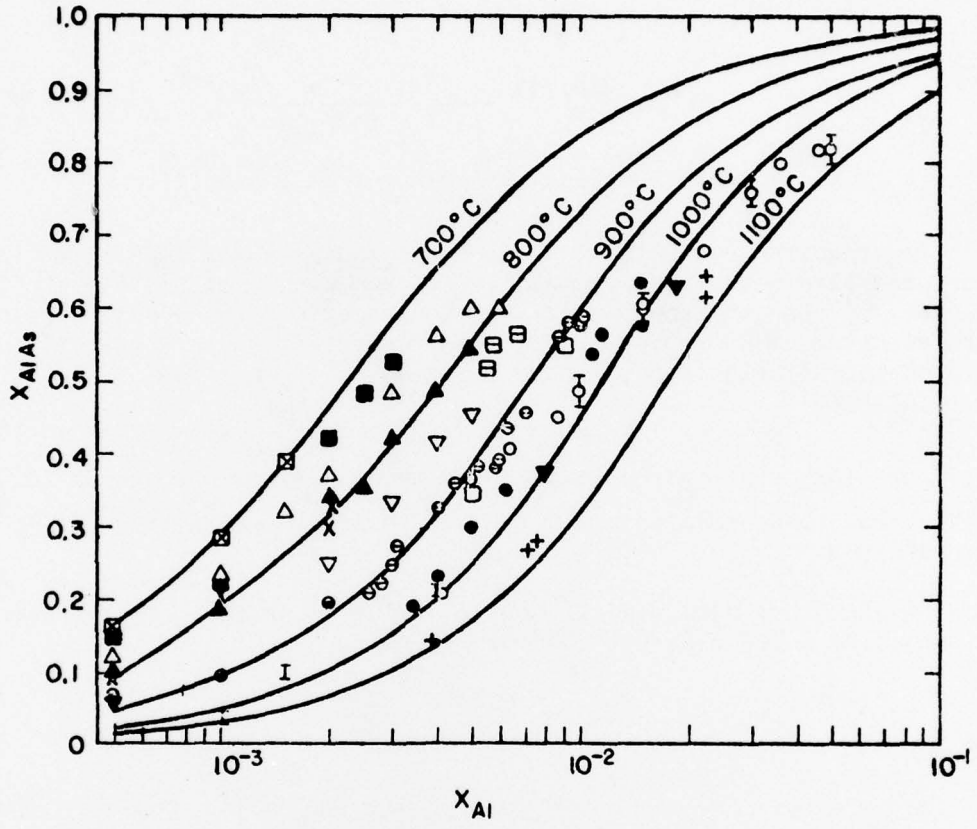

FIG. 18 Solidus section of the Al, Ga, As ternary phase diagram after Panish and Ilegems (ref 7).

REFERENCES

1. H. T. Minden, "Effects of proton bombardment on the properties of GaAs laser diodes", J. Appl. Phys. vol. 47, p. 1090, (1976).

2. R. Logan, private communication.

3. H. Minden, unpublished work.

4. Third Quarterly Report.

5. H. T. Minden, "A quartz sliding boat for GaAs liquid phase epitaxy", J. Crystal Growth, vol. 23, p. 79, (1974).

6. H. Minden, unpublished work.

7. M. B. Panish, S. Sumski, and I. Hayashi, "Preparation of multilayer LPE heterostructures with crystalline solid solutions of $Al_xGa_{1-x}As$: Heterostructure lasers", Met. Trans. AIME, vol. 2, p. 795, (1971).

8. H. T. Lockwood and M. Ettenberg, "Thin solution multiple layer epitaxy", J. Crystal Growth, vol. 15, p. 81, (1972).

9. J. J. Hsieh, "Thickness and surface morphology of GaAs LPE grown by supercooling, step-cooling, equilbrium-cooling, and two phase solution techniques", J. Grystal Growth, vol 27, p. 49, (1974).

10. R. N. Hall, "Solubility of III-V compound semiconductors in column III liquids", J. Electrochem Soc., vol. 110, p. 386, (1963).

11. M. B. Panish and M. Ilegems, "Phase equilibria in ternary systems", Progress in Solid State Chemistry, H. Reiss and J. O. McCaldin eds., Pergamon, Oxford, p. 65.

12. H. C. Casey and M. B. Panish, "The influence of the electrical properties of the solid phase on impurity incorporation during crystal growth", J. Crystal Growth, vol. 13/14, p. 820, (1972).

13. H. T. Minden, and R. Premo, "High temperature GaAs single heterojunction laser diodes", J. Appl. Phys., vol. 45, p. 4520, (1974).

14. F. E. Rosztoczy, F. Ermanis, I. Hayashi, and B. Schwartz, "Germanium doped gallium arsenide", J. Appl. Phys., vol. 41, p. 264, (1970).

MISSION
of
Rome Air Development Center

RADC plans and conducts research, exploratory and advanced development programs in command, control, and communications (C^3) activities, and in the C^3 areas of information sciences and intelligence. The principal technical mission areas are communications, electromagnetic guidance and control, surveillance of ground and aerospace objects, intelligence data collection and handling, information system technology, ionospheric propagation, solid state sciences, microwave physics and electronic reliability, maintainability and compatibility.

Printed by
United States Air Force
Hanscom AFB, Mass. 01731